PREDICTION OF PV MODULE NOMINAL OPERATING CELL TEMPERATURE USING ELECTROMAGNETIC WAVE MODELING

Biao Li, Matthias Duell, Tanja Schuhmacher, Dan M. J. Doble
Fraunhofer Center for Sustainable Energy Systems, 25 1st Street, Cambridge, MA 02141

ABSTRACT

Nominal operating cell temperature, NOCT, defined by module heat generation and loss mechanisms, is an important factor relating to energy conversion efficiency of PV modules. Development of simulation tools for predicting NOCT is an important element of designing modules that may function to operate at lower NOCT. When modeling the heat generation from incoming radiation, it is highly desirable to accurately simulate the solar energy conversion in the cell, glass, encapsulant and anti-reflective layers, as well as the spaces between the cells. We present herein an approach that starts from the fundamental of electromagnetic wave (EMW) propagation based on Maxwell's equations. This approach enables the EMW energy in individual layers and at different regions of the PV module to be evaluated from the dielectric constants and thickness of each material. Once the light intensity in the cell is known, it becomes possible to predict cell electrical parameters using established electrical models. This methodology was applied to a packaged back-junction-back-contact (BJBC) cell and compared with parameters derived from an experimental I-V curve. Good agreement was observed for both electrical parameters and external quantum efficiency. The distribution of solar energy conversion within the module was further combined with heat transfer and 3D finite element analysis models to enable a prediction of thermal profiles of the module. The simulated temperature distribution was found to agree well with experimental measurements using a thermal imaging camera and thermocouples.

INTRODUCTION

Reducing nominal operating cell temperature (NOCT) in modules is one approach to improving PV module energy yield. Under steady state conditions, the NOCT is determined by the equilibrium between the heat generation in the module and heat loss to the environment. Although module heat loss via conduction, convection and radiation is well understood by theoretical models [1] the study the heat generation in the PV module warrants further investigation. A general assumption often applied is that if the efficiency of solar cell is η, then $(1-\eta)$ of solar energy will be converted to heat. In reality, heat is generated non-uniformly with the various layers and regions each absorbing a portion of the incoming radiation.

We present herein an approach to evaluate electromagnetic wave (EMW) propagation in individual layers and at different regions of the PV module. Once the light intensity in the cell is known, it becomes possible to predict cell electrical parameters using established electrical models. The distribution of solar energy conversion within the module was further combined with heat transfer and 3D finite element analysis models to enable a prediction of thermal profiles of the module. The experimental results show that the EMW model is capable of predicting both electrical and thermal performance of the PV module.

MODELING AND SIMULATION OF NOCT

EMW modeling

Fig 1a shows a crystalline silicon PV module, consisting of cell and street regions. Electromagnetic wave propagation in two regions is different, as shown in Fig 1b, due to significant discrepancy of the medium.

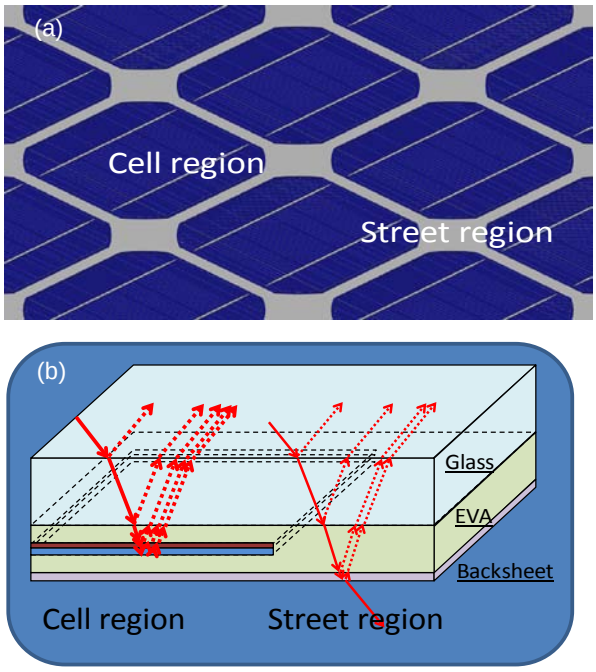

Figure 1 (a) SolidWorks model of a PV module. (b) Diagram of EMW distribution in the module.

In order to quantitatively evaluate the solar energy conversion in different regions, Maxwell's equations were used to predict the EMW propagation within the module. Based on continuity requirements of the electric (E) and magnetic (B) fields across boundaries from one medium to the next, the magnitude of fields at the top interface of i-th dielectric layer, E_i and B_i, is simply related to the bottom interface of the same layer, E_{i+1} and B_{i+1}, through the matrix relation [2]:

$$\begin{pmatrix} E_i \\ B_i \end{pmatrix} = M_{i+1} \begin{pmatrix} E_{i+1} \\ B_{i+1} \end{pmatrix} = \begin{pmatrix} \cos\delta & \frac{i}{\gamma}\sin\delta \\ i\gamma\sin\delta & \cos\delta \end{pmatrix} \begin{pmatrix} E_{i+1} \\ B_{i+1} \end{pmatrix} \quad (1)$$

Where $\gamma = \sqrt{\epsilon/\mu}$, ϵ and μ are the dielectric constant and magnetic permeability, respectively. The phase change $\delta = {2\pi\tilde{n}(\lambda)d}/{\lambda}$, where d is layer thickness. The wavelength-dependent complex refractive index $\tilde{n}(\lambda) = n(\lambda) - ik(\lambda)$. As a consequence, the PV module consisting of sequence of N dielectric layers can be represented as a system matrix, which is the product of the individual layer matrices as.

$$\begin{pmatrix} E_0 \\ B_0 \end{pmatrix} = M_1 M_1 \ldots M_N \begin{pmatrix} E_N \\ B_N \end{pmatrix} = \begin{pmatrix} M_{11}(\lambda) & M_{12}(\lambda) \\ M_{21}(\lambda) & M_{22}(\lambda) \end{pmatrix} \begin{pmatrix} E_N \\ B_N \end{pmatrix} \quad (2)$$

where M_i is the transfer matrix of the i-th layer, E_0 and B_0 are the electric and magnetic field amplitudes at the first interface, E_N and B_N the field amplitudes at the last interface. The elements in the system matrix, $M_{\alpha\beta}(\lambda)$, are wavelength dependent. The reflection and transmission coefficient can then be derived as

$$r(\lambda) = \frac{M_{11}(\lambda)\tilde{n}_0 + M_{12}(\lambda)\tilde{n}_0\tilde{n}_N - M_{21}(\lambda) - M_{22}(\lambda)\tilde{n}_N}{M_{11}(\lambda)\tilde{n}_0 + M_{12}(\lambda)\tilde{n}_0\eta_N + M_{21}(\lambda) + M_{22}(\lambda)\tilde{n}_N} \quad (3a)$$

$$t(\lambda) = \frac{2\tilde{n}_0}{M_{11}(\lambda)\tilde{n}_0 + M_{12}(\lambda)\tilde{n}_0\tilde{n} + M_{21}(\lambda) + M_{22}(\lambda)\tilde{n}} \quad (3b)$$

The reflectance R and transmittance T are given by $R(\lambda) = |r(\lambda)|^2$ and $T(\lambda) = |t(\lambda)|^2$, respectively. Fig 2 shows the measured and calculated transmission spectra for a single layer of back sheet and EVA encapsulant, respectively. It is seen that EVA is very transparent except in the UV range, while backsheet is capable of absorbing a large amount of light. Through calculation the wavelength dependent refractive index of different materials can be derived.

The key feature of the EMW model is that EMW distribution in individual layers of PV module can be modeled and evaluated. According to Ref [3], the electric field on the k-th interface can be expressed as,

$$E_k(\lambda) = \lfloor 1 + r(\lambda) \rfloor m_{22}^{(k)}(\lambda) - \gamma_0 \lfloor 1 - r(\lambda) \rfloor m_{12}^{(k)}(\lambda) \quad (4)$$

Where $m_{\alpha\beta}^{(k)}(\lambda)$ are the elements of the transfer matrix from the first to the k-th interface. The intensity is then simply the square of the electric field, as plotted in Fig 3 for the PV module in cell and street regions, respectively.

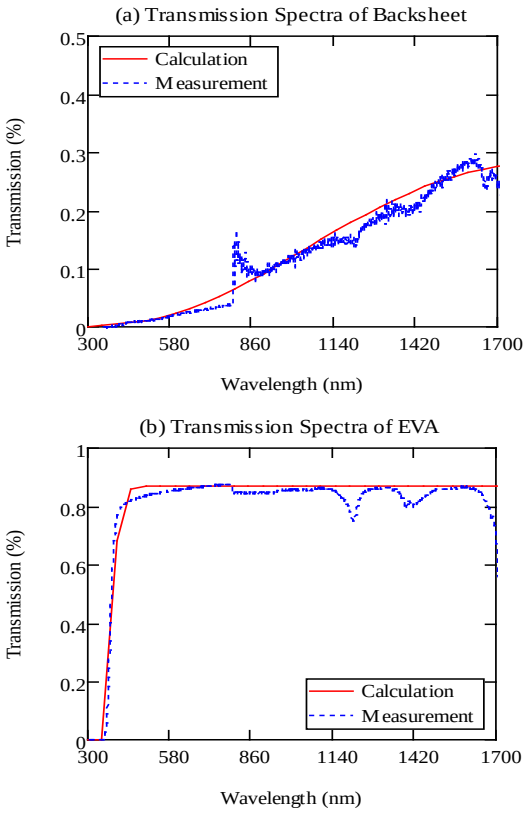

Figure 2: Measured and calculated transmission spectra for a single layer of (a) backsheet and (b) EVA encapsulant, respectively.

The light intensity distribution as predicted from the EMW model can be combined with the solar spectrum, $I_{sun}(\lambda)$, to predict the power dissipated in each layer, P_k, of the PV module as

$$P_k = \frac{\int I_{sun}(\lambda)|E_k(\lambda)|^2 d\lambda}{\int I_{sun}(\lambda) d\lambda} \quad (5)$$

Eqs. (1) to (5) can be used to predict heat generation in encapsulant and backsheet materials. As for solar cell in the PV module, partial of the absorbed energy is used to produce electricity, the rest is converted to heat. Once the magnitude of electric filed in the cell $|E_{cell}|^2$ is evaluated from Eqs. (1) to (4), it becomes possible to predict the electrical performance of the cell in the module using established electrical models. The external quantum efficiency can be derived as

$$EQE(\lambda) = \int \alpha(\lambda)\lfloor 1 - R(\lambda) \rfloor |E_{cell}(\lambda)|^2 e^{-\alpha x} \eta c(x) dx \quad (6)$$

Where $\alpha(\lambda)$ is the absorption coefficient of cell, $\eta c(x)$ is the spatial collection efficiency [4]. The short-circuit current,

open-circuit voltage, filled factor and efficiency of the cell can then be calculated as [5]

$$J_{sc} = \frac{\int I_{sun}(\lambda)|E_{cell}|^2 EQE(\lambda)\lambda/\lambda_{cell} d\lambda}{\int I_{sun}(\lambda) d\lambda} \quad (7a)$$

$$V_{oc} = \frac{nkT}{q} ln(J_{sc}/J_0 + 1) \quad (7b)$$

$$FF = \frac{V_{oc} - \ln(V_{oc} + 0.72)}{V_{oc} + 1} \quad (7c)$$

$$\eta = \frac{V_{oc} I_{sc} FF}{\int I_{sun}(\lambda) d\lambda} \quad (7d)$$

Where λ_{cell} is the cut-off wavelength of the cell, T, the junction temperature, J_0, the saturation current, n, the ideality factor, and q, the electronic charge.

Due to thermalization, recombination and Joule heat effect [6], (1-η) percentage of solar irradiation absorbed by cell is converted to heat. The total amount of heat produced by cell is expressed as

$$Heat_{cell} = \frac{\int I_{sun}(\lambda)|E_{cell}(\lambda)|^2(1-\eta) d\lambda}{\int I_{sun}(\lambda) d\lambda} \quad (8)$$

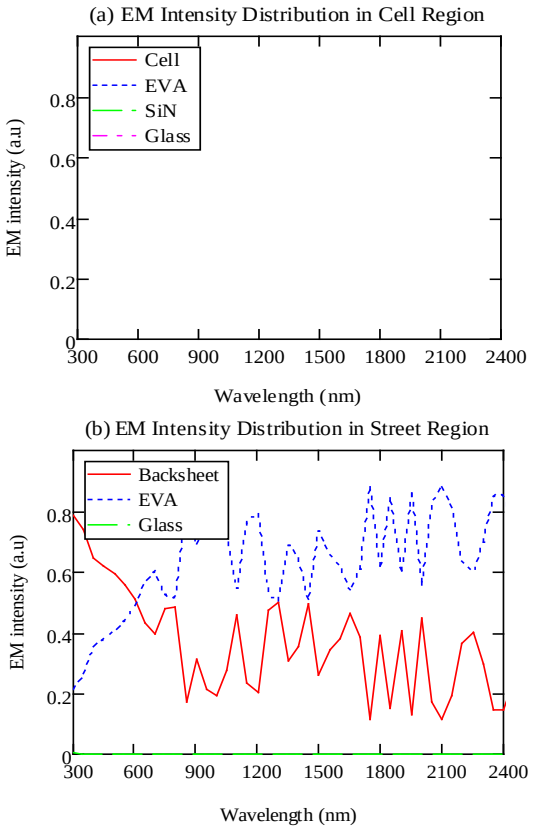

Figure 3: Calculated EMW intensity distribution in (a) cell and (b) street regions.

Figure 4 shows the calculated energy distribution within individual layers of the module under standard global AM 1.5 illumination conditions. The spectral average of energy production is exhibited in the legends. Assuming 17.3% PV conversion efficiency of solar cell at 25 °C and normal incidence, the EMW model predicts that 149 W/m^2 solar irradiation is converted to electricity at operating temperature of 65 °C, approximately 80 W/m^2 energy reflects back to ambient, 678 W/m^2 heat is produced in cell due to thermoionization and free carrier absorption, and 91 W/m^2 heat is generated in encapsulant due to the absorption of EVA especially in the UV range. While in the street region, heat generation depends on the type of backsheet material. In our case, approximately one third of solar irradiance transmits through the module, the rest is absorbed by encapsulant and backsheet to generate heat.

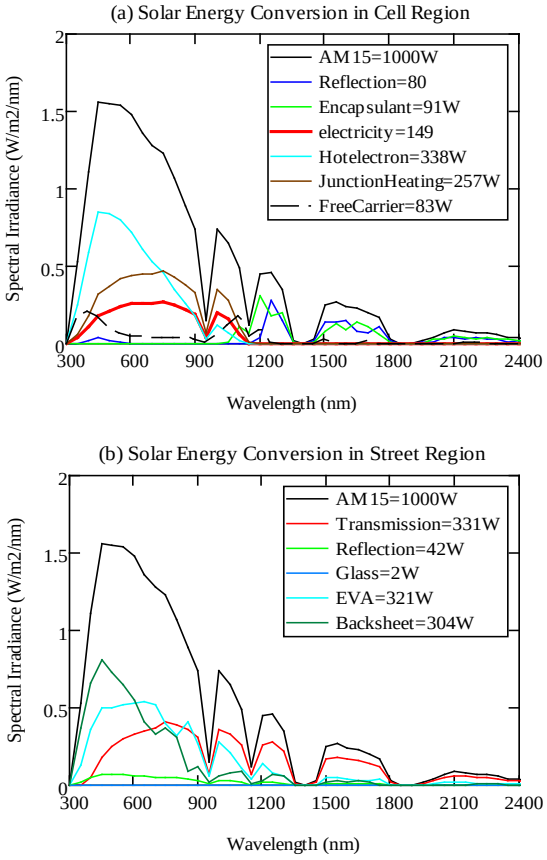

Figure 4: Breakdown of solar energy conversion in (a) cell and (b) street regions of the PV module

Finite element modeling

The EMW model has also been used to predict the temperature distribution in a module. In addition to the results of the EMW simulation, several other factors must be included: the solar spectrum, thermal resistance of

individual layers, convective and conductive cooling, cell efficiency, optical properties of materials and packing density of cells. It is a three dimensional problem which can be solved through finite element analysis (FEA), provided that heat flow in the module can be well defined.

The EMW simulation predicts that 91 W/m^2 is generated in encapsulant, 80 W/m^2 is reflected back to ambient. Assuming that this is constant then the heat generated in cell can be estimated as 1000*(1-η)-91-80 W/m^2. Fig 5a shows an exploded view of the FEA model with different heat flow produced in different layers at cell and street regions of the PV module, respectively. In addition to heat generation, NOCT of the module is also closely related to the thermal properties of individual layer. Fig 5b exhibits the calculated thermal resistance between layers. The thermal barrier for transferring heat across the module surface is significant. This implies that the reduction of surface thermal resistance is a critical approach to lowering NOCT.

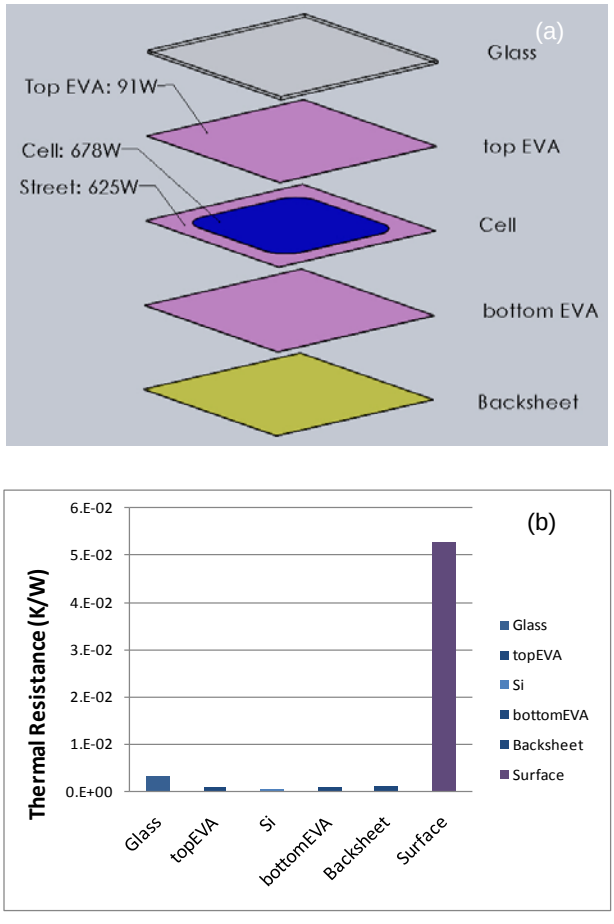

Figure 5: (a) Exploded view of a FEA model with different heat flow generated in cell and encapsulant at different regions, respectively. (b) Calculated thermal resistance between layers in the module.

EXPERIMENTAL VERIFICATION

Electrical testing of a BJBC module

A back-junction-back-contact (BJBC) module has been assembled for electric test. Fig. 6 shows the external quantum efficiency of the module as a function of wavelength. Dotted line represents the experimental result, while line is the calculated profile from Eqs. (1) to (4) and (6). Table I lists the cell parameters derived from an experimental I-V curve and EMW modeling. Good agreement was observed for both electrical parameters and external quantum efficiency.

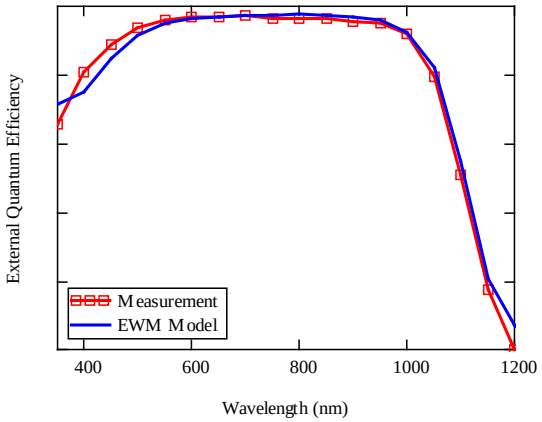

Figure 6: Measured and calculated quantum efficiency for a BJBC module

	Jsc (mA/cm2)	Voc (mV)	FF (%)	η (%)
Measurement	38.112	647.300	73.700	18.182
EMW modeling	40.069	642.783	73.537	18.940

Table 1: Measured and calculated electrical parameters for the BJBC module

Thermal testing of a mini-module

The predicted temperature distribution within a module was compared with experimental data. Mini modules with four integrated thermocouples were assembled specifically for thermal study. The first thermocouple was attached directly on the cell, the second within the EVA beside a cell, the third and fourth was attached to the backsheet at the center and edge respectively. A DAQ system was setup to record the temperature profiles. The module is clamp fixed under a sun simulator for solar exposure test, as shown in Fig 7. Additionally, an infrared thermal imaging camera was used for measurement of glass surface temperature.

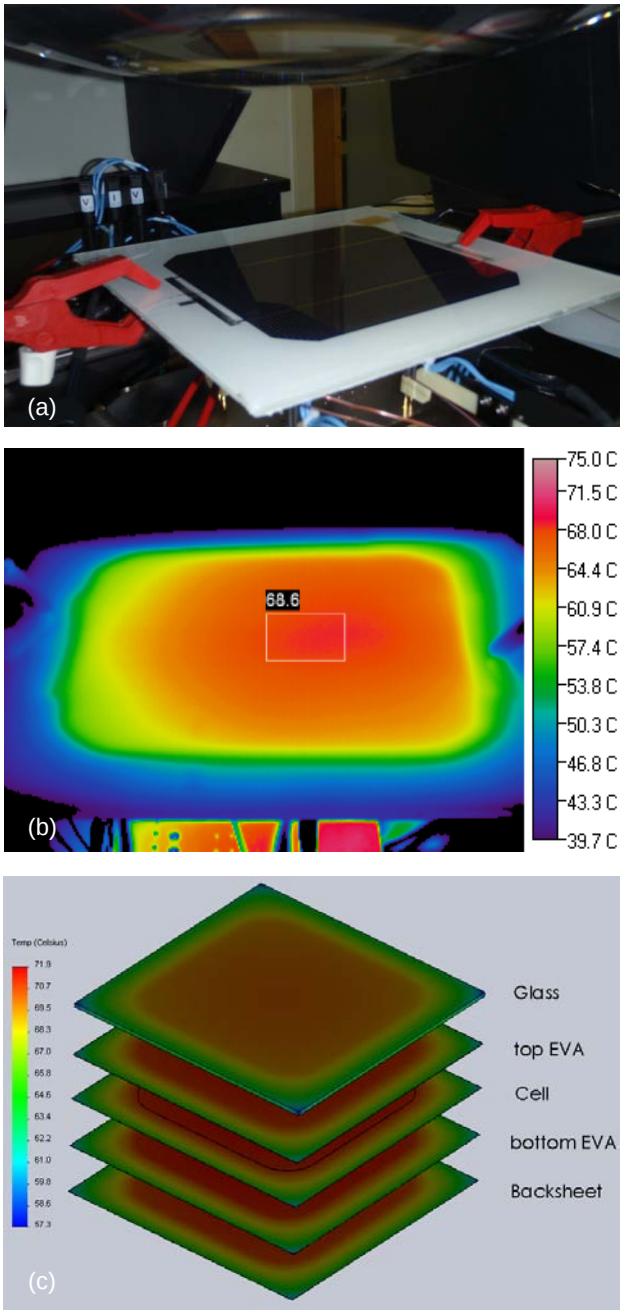

Figure 7: (a) A fabricated mini module with integrated thermal couples for solar exposure test. (b) Thermography and (c) FEA simulation of module temperature after 30 mins exposure to sun simulator.

Shown in Fig 7b is the thermography of the module after 30 mins exposure to sun simulator. The surface temperature of glass is measured as 68.6 ^{o}C. Fig. 7c displays the FEA modeling of temperature distribution in individual layer of the module. Heat generation in the model is assigned based on EMW modeling results as shown in Fig. 5a. It is seen that the simulated glass surface temperature, 69^{o}C, is slightly lower than cell temperature, 72^{o}C. The FEA model agrees well with measurement using build-in thermocouples.

Furthermore, the dynamic temperature profiles of the module after the light was switched on and off were recorded and compared with results from the FEA thermal simulation. Fig 8 shows the measured and simulated temperature profiles of cell and encapsulant, respectively, which corresponds to cell and street regions in Fig. 1. It is seen that the temperature in cell region is about 9^{o}C higher than that in street region for the mini-module. Time constant of heating is approximately 380 s in both regions. The simulation coincides well with the measurement, indicating that the heat flow evaluation based on EMW model is applicable for 3D finite element analysis.

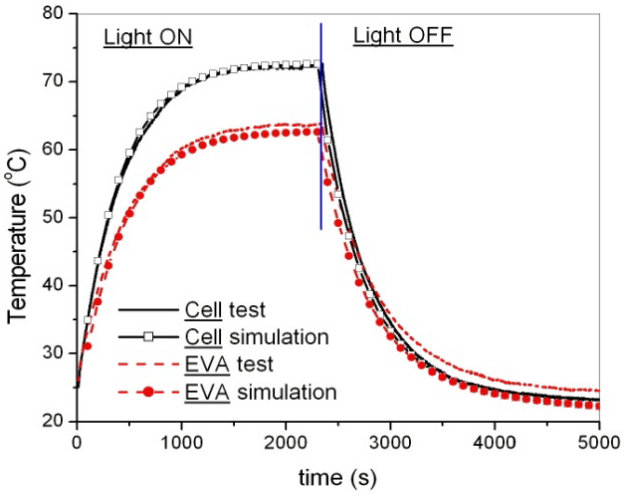

Figure 8: Measured and simulated temperature profiles of cell and encapsulant inside the module, respectively.

PREDICTION OF NOCT IN PV MODULE

The EMW model can be extended to predict lateral temperature distribution within a PV module. Figure 9 shows the EMW generated and experimentally observed thermal image of a PV module after 1 hour outdoor exposure to sunlight. The same colors are used in each profile. The street region appears more distinct in the EMW model due to the relatively large size of the elements. Thermography image shows that the temperature of the glass surface in the cell and street regions is 60.4 ^{o}C and 58.7 ^{o}C respectively. This agrees well with EMW model prediction of the glass surface temperature, 60.8 ^{o}C in cell region and 57.4 ^{o}C in the street region.

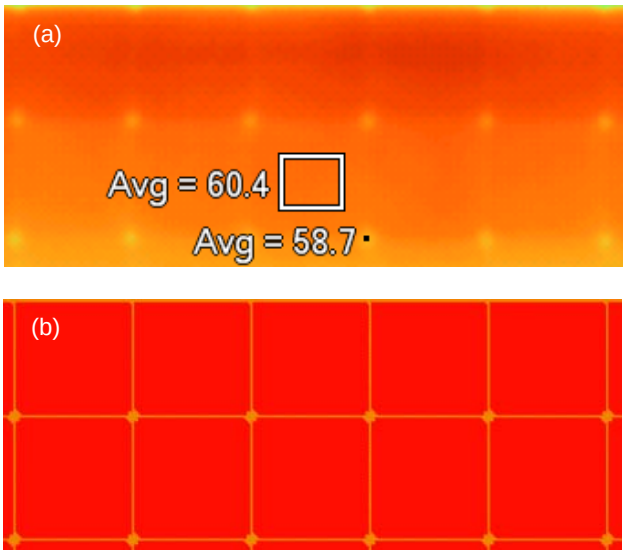

Figure 9: Temperature mapping of a PV module after 1 hour outdoor exposure to sun obtained from (a) thermal imaging and (b) EMW model. The same colors are used in each profile. The street region appears more distinct in the EMW model due to the relatively large size of the elements.

CONCLUSION

In summary, the EMW energy in individual layers and at different regions of the PV module has been evaluated. This enabled an accurate prediction of solar energy conversion in the module. The simulated NOCT was found to agree well with indoor and outdoor measurements. Our investigation would assist in innovating module design and optimizing thermal management.

REFERENCES

[1] S.C.W. Krauter, *Solar Electric Power Generation*, Springer Berlin Heidelberg (2006)

[2] F. L. Pedrotti, L. M. Pedrotti and L. S. Pedrotti, *Introduction to Optics*, Prentice-Hall, Englewood Cliffs, NJ(2006)

[3] Luca Dal Negro, C. Oton, Z. Gaburro, L. Pavesi, P. Johnson, A. Lagendijk, R. Righini, M. Colocci, and D. Wiersma, "Light transport through the band-edge states of Fibonacci quasicrystals", *Physical Review Letters*, **90**, 2004, 055501

[4] P. Kittidachachan et al, "A detailed study of p-n junction solar cells by means of collection efficiency", *Solar Energy Materials & Solar Cells*, **91**, 2007, 160

[5] M.A. Green, "Accuracy of analytical expressions for solar cell fill factors", *Solar Cells*, **7**, 1982, 337-340.

[6] O. Breitenstein, J. Rakotoniaina, Electrothermal simulation of a defect in a solar cell", *Journal of Applied Physics*, **97**, 2005, 074905.